Thermodynamic Stability of β-Peptide Helices and the Role of Cyclic Residues

Nitin Rathore,* Samuel H. Gellman,† and Juan J. de Pablo‡
*Novozymes North America, Franklinton, North Carolina; and †Department of Chemistry, ‡Department of Chemical and Biological Engineering, University of Wisconsin-Madison, Madison, Wisconsin

ABSTRACT Beta-peptides are emerging as an attractive class of peptidomimetic molecules. In contrast to naturally occurring α-peptides, short oligomers of β-amino acids (comprising just 4–6 monomers) exhibit stable secondary structures that make them amenable for quantitative, concerted experimental and theoretical studies of the effects of particular chemical interactions on structure. In this work, molecular simulations are used to study the thermodynamic stability of helical conformations formed by β-peptides containing varying proportions of acyclic (β^3) and cyclic (ACH) residues. More specifically, several β-peptides differing only in their content of cyclic residues are considered in this work. Previous computational studies of β-peptides have relied mostly on energy minimization of molecular dynamics simulations. In contrast, our study relies on density-of-states based Monte Carlo simulations to calculate the free energy and examine the stability of various folded structures of these molecules along a well-defined order parameter. By resorting to an expanded-ensemble formalism, we are able to determine the free energy required to unfold specific molecules, a quantity that could be measured directly through single-molecule force spectroscopy. Simulations in both implicit and explicit solvents have permitted a systematic study of the role of cyclic residues and electrostatics on the stability of secondary structures. The molecules considered in this work are shown to exhibit stable H-14 helical conformations and, in some cases, relatively stable H-12 conformations, thereby suggesting that solvent quality may be used to manipulate the hydrogen-bonding patterns and structure of these peptides.

INTRODUCTION

Synthetic oligomers designed to emulate the structural and functional properties of natural peptides and proteins are emerging as promising subjects for basic research (1–3). β-Peptides, oligomers of β-amino acids, represent a particularly well-studied class of unnatural foldamers (4,5). β-Amino acids contain one additional backbone carbon atom (see Fig. 1) relative to the α-amino acids found in proteins. β-Peptides have been shown to display high folding propensities relative to α-peptides of comparable length. For example, β-peptides containing as few as six residues adopt helical conformations in water if the residues are properly selected (6–8), while α-peptides must typically be two or three times longer to display significant helicity (9). β-Peptides appear to form a larger variety of secondary structures than do α-peptides (4,5). Only two hydrogen-bonded helices are known among α-peptides (α and 3_{10}), while at least five have been reported among β-peptides.

The β-peptides' folding propensity can be controlled by manipulating the substitution pattern of the β-amino-acid residues. For example, β-amino-acid residues bearing a single side chain, adjacent to the nitrogen (β^3-residues), tend to adopt a helix defined by 14-membered ring hydrogen bonds (C=O (i) – H-N ($i-2$)), termed the ''14-helix'' (4,5). The folding propensity of β^3-residues is only moderate, however; residues with a six-membered ring constraint, e.g., *trans*-2-aminocyclohexanecarboxylic acid (ACHC) residues, display a much stronger 14-helical propensity (6,10). Residues with a five-membered ring constraint adopt a different secondary structure, the ''12-helix,'' which is defined by 12-membered ring hydrogen bonds (C=O (i) – H-N ($i+3$)) (11). The nomenclature employed in this work uses the term ''H-14'' helix to denote a helix with 14-member hydrogen bonds, and ''H-12'' to denote a helix with 12-membered hydrogen bonds. The potential to program well-defined folding patterns into β-peptide molecules, coupled to their resistance to proteolytic degradation (12), has spawned a number of efforts to explore a variety of biomedical applications for these foldamers (13–18).

Experimental efforts aimed at characterizing the conformation of β-peptides have often resorted to circular dichroism. As shown in this work, conventional circular dichroism experiments cannot probe the simultaneous existence of various types of folded β-peptide conformations, and fail to provide a level of resolution that is commensurate with the degree of control that can be currently achieved in the synthesis of these molecules. Synthetic efforts aimed at producing and characterizing various β-peptides have therefore benefitted from parallel computational studies aimed at elucidating the origins and validity of empirical correlations between β-amino-acid substitution pattern and β-peptide folding. Wu and Wang (19) used energy-minimization calculations to evaluate the relative stability of a β-sheet, an H-14 helix, and an H-12 helix in model β-dipeptides and β-hexapeptides. Van Gunsteren and co-workers used molecular dynamics simulations and the GROMOS96 biomolecular

Submitted March 5, 2006, and accepted for publication July 24, 2006.

Address reprint requests to J. J. de Pablo, Tel.: 608-262-7727, E-mail: depablo@engr.wisc.edu.

0006-3495/06/11/3425/11 $2.00 doi: 10.1529/biophysj.106.084491

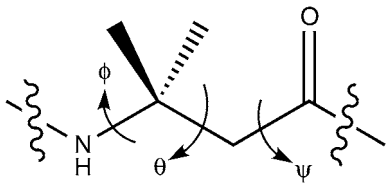

FIGURE 1 Chemical structure of a β-amino-acid residue, with identification of key torsion angles.

force field to study folding and unfolding transitions for several β-peptides (20–22) and, more recently, to investigate the role of side-chain branching on folding behavior (23). Hofmann and co-workers performed energy-minimization calculations (24) and thermodynamic integration (25,26) using the CHARMM23.1 molecular mechanics force field to explore several periodic structures of β-peptides. A different force field, OPLS-AA (27), was employed in molecular dynamics simulations by Jorgensen and co-workers to study β-peptides (28) and to investigate the role of side-chain structure on H-14 helicity (29).

It is important to emphasize that past computational studies of β-peptides have relied exclusively on potential energy-minimization or molecular dynamics approaches. As a result, little is known about the free energy landscape of these molecules. Potential energy minimization calculations using interactions generated by means of electronic-structure methods have been limited to very short peptides of fewer than six amino acids. Perhaps more importantly, potential energy-minimized structures do not necessarily correspond to free energy minima, and it is therefore unclear whether the structures considered in past studies were thermodynamically stable. As mentioned above, molecular dynamics simulations have also been used to examine relatively short trajectories of β-peptides. Such simulations are limited to the study of relatively fast (nanosecond scale) processes and can suffer from sampling inefficiencies. The results of Monte Carlo simulations presented in this work show that some of the free energy barriers that separate local free energy minima could be sufficient to trap a conformation in a metastable conformation over the entire span of a long molecular dynamics simulation. Past computational studies of β-peptides have not been conclusive in demonstrating the validity of empirically determined correlations between their chemical structure and conformation. There is ample room for improvements both in force-field parameters and in the methods employed to characterize theoretically and experimentally the stable and meta-stable conformations of these molecules.

Over the past few years, single-molecule force spectroscopy has emerged as a promising new technique for characterization of the folding processes and biological molecules, including large proteins and DNA (30–32). We believe that our understanding of β-peptides could be enhanced considerably by force spectroscopy measurements. With this aim in mind, in this work we examine the free energy required to unfold specific β-peptides that have already been synthesized in our laboratories by pulling on their ends. The free energy generated in this manner could subsequently provide the basis for transition-path ensemble simulations of the actual folding process. The simulations presented in this work have resorted to a novel Monte Carlo algorithm capable of generating high accuracy estimates of the free energy landscape of a system as a function of one or more order parameters. These simulations also represent the first calculations of the structure and free energy of β-peptides with cyclic side chains. In contrast to past modeling studies of β-peptides, we use a combination of molecular dynamics and density-of-states based Monte Carlo simulations to improve sampling of phase space, thereby arriving at reliable estimates of the thermodynamic stability of the helical conformations adopted by these molecules. An all-atom representation is adopted, with CHARMM-like force field parameters. The solvent is treated explicitly for the molecular dynamics runs, and as a continuum for Monte Carlo and several longer molecular dynamics calculations. In agreement with experiments (6,33,34), our simulations show that the use of cyclic constraints, as in amino-cyclo-hexane-carboxylic acid (ACHC), greatly enhances H-14 helicity in β-peptides. Simulations in a continuum also suggest that electrostatic interactions play an important role in the stability of these oligomers. The β-peptides, especially those without cyclic constraints, are shown to exhibit 12-membered hydrogen bonding (in addition to H-14 helices) in a low dielectric environment. The relative stability of these two helices is shown to depend on the dielectric of the medium, suggesting that solvent quality could be exploited to manipulate the secondary structure of these molecules. Perhaps more importantly, our results provide a clear motivation and a framework for using mechanical stretching (force-extension plots) to characterize H-14 and H-12 helices. These conformations differ significantly in their optimal lengths, and their existence and stability can be probed unambiguously by single-molecule pulling experiments.

MODEL AND METHODS

Protein model

We used an-all atom representation for the peptides considered in this work. Based on the cyclic residue content, these peptides belong to three classes:

Acyclic: Homo-oligomers of β-alanine, $[\beta^3\text{hAla}]_{12}$ and $[\beta^3\text{hAla}]_9$.
One-third cyclic: nine-residue hetero-oligomers, $[\text{ACHC-}\beta^3\text{Lys-}\beta^3\text{Leu}]_3$ and $[\text{ACHC-}\beta^3\text{hAla-}\beta^3\text{hAla}]_3$.
Cyclic: nine-residue homo-oligomer of amino-cyclo-hexane-carboxylic acid $[\text{ACHC}]_9$.

While the majority of our calculations were performed on the three peptides depicted in Fig. 2, some of the implicit-solvent simulations were also performed on $[\beta^3\text{hAla}]_9$ and $[\text{ACHC-}\beta^3\text{hAla-}\beta^3\text{hAla}]_3$ to achieve chain-length and residue consistency. The interaction parameters employed in this work were assigned in accordance with the CHARMM27 force field (35). It should be noted that no standard CHARMM parameters are available for β-amino-acid residues. The parameters were therefore assigned based on

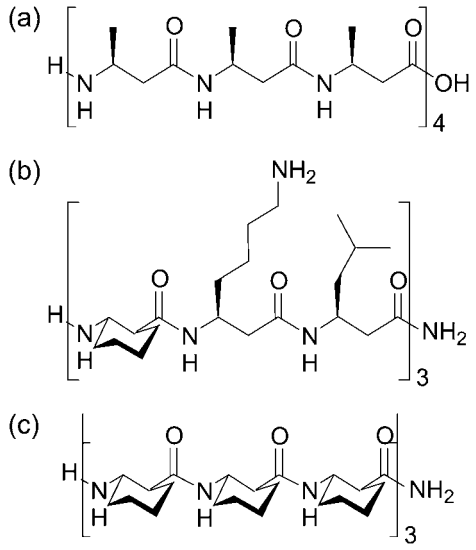

FIGURE 2 Chemical structure of three of the β-peptides studied in this work: (*a*) $[\beta^3\text{hAla}]_{12}$; (*b*) [ACHC-$\beta^3$Lys-$\beta^3$Leu]$_3$; and (*c*) $[\text{ACHC}]_9$.

similarity to the chemical structures of the molecules for which standard CHARMM parameters are available. (These force-field files are available from the authors.) The interactions between atoms are described by the following potential energy function:

$$U_{\text{total}} = \sum_{\text{bonds}} K_r(r - r_{\text{eq}})^2 + \sum_{\text{angles}} K_\theta(\theta - \theta_{\text{eq}})^2 + \sum_{\text{dihedrals}} K_\phi[1 + \cos(n\phi - \delta)] + \sum_{\text{impropers}} K_\omega(\omega - \omega_{\text{eq}})^2 + \sum_{\text{LJ}} \varepsilon_{ij}\left[\left(\frac{\sigma_{ij}}{r_{ij}}\right)^{12} - 2\left(\frac{\sigma_{ij}}{r_{ij}}\right)^{6}\right] + \sum_{\text{Coulombic}} \frac{1}{4\pi\varepsilon(r)\varepsilon_o}\frac{q_i q_j}{r_{ij}}. \quad (1)$$

A 1–3 exclusion principle was used for the nonbonded energy, and the 1–4 Coulomb interactions were scaled down by a factor of 0.4. A cutoff of 10 Å was used for both the electrostatic and van der Waals terms. A simple force-shift scheme was employed for Coulombic interactions in a continuum solvent, while for simulations in explicit solvent we used a smooth particle-mesh Ewald technique (36). A simple cut-and-shifted potential was employed for Lennard-Jones interactions.

Solvent treatment

Two different approaches were employed to describe solvent effects. First, MD runs for the three peptides were performed in explicit solvents. Methanol was used as a solvent for acyclic $[\beta^3\text{h-Ala}]_{12}$, whereas $[\text{ACHC}]_9$ and [ACHC-β^3Lys-β^3Leu]$_3$ (with neutral side chains) were studied in water. The CHARMM model parameters were used for methanol, and the TIP3P model (37) was used for water. Periodic boundary conditions were employed in the three directions, and electrostatic interactions were computed through a smooth particle-mesh Ewald method (36). These explicit solvent molecular dynamics simulations were conducted for up to 10 ns for each of the test molecules considered in this study.

Second, long MD runs and Monte Carlo simulations were also performed in a distance-dependent dielectric continuum. A force-shift scheme was used for electrostatic interactions; the potential energy, as well as the forces, goes to zero at the cutoff distance. The modified potential for the Coulombic interactions is given by

$$U_{\text{Coulombic}} = \sum \frac{1}{4\pi\varepsilon(r)\varepsilon_o}\frac{q_i q_j}{r_{ij}} \times \left(1 - 2\frac{r_{ij}^2}{r_c^2} + \frac{r_{ij}^4}{r_c^4}\right), \quad (2)$$

where r_{ij} is the separation between point charges i and j and r_c is the cutoff radius. The distance-dependent dielectric (38,39) was modeled as a linear function of separation between two point charges, $\epsilon = \epsilon(r) = \alpha r$. Different values of α (1, 1.2, 1.5, 2.0) were considered in this study to explore the effect of polarity of the solvent on the secondary structure exhibited by different β-peptides.

Simulation methods

Molecular dynamics

Molecular dynamics simulations using a multiple time-step algorithm (40) were conducted with a short time step of 0.5 fs. The crystal structure of $[\text{ACHC}]_6$ was used to generate the model H-14 scaffold for the peptides. Low-dielectric gas phase simulations of the peptides with acyclic residues (acyclic, Fig. 2 *a*; and one-third cyclic, Fig. 2 *b*) also yielded H-12 helices. MD simulations were also conducted starting from these two model helical conformations, H-14 and H-12. Root mean-square deviations based on the C_α atoms were calculated for the MD trajectories. To better characterize these helices, we monitored the number of intramolecular 14-membered and 12-membered hydrogen bonds being formed by the peptide during the simulations.

Expanded ensemble density of states (EXEDOS)

In addition to the MD runs, expanded ensemble density-of-states (EXEDOS) Monte Carlo simulations were conducted in this work. Different types of trial moves were employed. The first type consisted of hybrid molecular dynamics/Monte Carlo displacements; the second type consisted of nonlocal pivot attempts, and the third move consisted of a local random displacement of a randomly selected amino-acid residue. Unlike molecular dynamics simulations, where sampling is generally limited to configurations in the vicinity of a local energy minimum, the EXEDOS method permits sampling of both H-12 and H-14 conformations and provides estimates of the free energy difference between distinct populations. In recent work (41,42), we have introduced EXEDOS implementations where intermediate states facilitate the transition between configurations separated by large energy barriers. The expanded states are usually defined by some reaction coordinate, ξ, and the sampling in ξ-space is governed by unknown weights that are determined on the fly as the simulation proceeds. The EXEDOS method has been employed for studies of suspensions of colloidal particles in liquid crystals (41) and for the reversible mechanical stretching of proteins (42). The reader is referred to the literature for technical details. In this work, the reaction coordinate, ξ, was chosen to be the end-to-end distance between the amino *N* of the second residue from the *N*-terminus and the carbonyl *C* of the second residue from the *C*-terminus. The two terminal residues are usually more free because of insufficient hydrogen bonding and hence, to minimize the noise, penultimate residues are used to define the reaction coordinate.

To facilitate convergence and sampling, the ξ-space was fragmented into smaller overlapping domains or windows. Multiple, noninteracting replicas of the peptide molecule were created and simulated in different boxes. Each simulation box corresponds to a window with a specific range of ξ, and these end-to-end distance ranges are assigned so that windows corresponding to adjacent boxes overlap with each other. In addition to implementing regular Monte Carlo moves, configurations in different boxes were swapped at regular intervals during the simulation. Swapping ensured that systems in individual windows did not get trapped in particular configurations as a result of the bounds imposed by the window size. The ability to simulate parallel replicas of the system gives the added advantage of speeding up the calculations by having each replica run on a separate processor.

Calculation of helicity

The conformations of β-peptides during simulation were quantified in terms of the root mean-square deviation from a model structure and helicity of the chains. The helicity of the peptides was computed in two different ways. In the first, a measure of helicity was obtained directly from the number of H-14 or H-12 hydrogen bonds. For example, the H-14 helicity of a conformation can be written as

$$Helicity_{\text{hbonds}} = \frac{N_{\text{H-14}}}{N_{\text{H-14}}^{\text{max}}}, \quad (3)$$

where $N_{\text{H-14}}$ is the number of 14-membered hydrogen bonds in the chain and $N_{\text{H-14}}^{\text{max}}$ is the maximum number of H-14 hydrogen bonds in a perfect H-14 helical conformation of the peptide chain. A similar measure was used to describe H-12 helicity.

A second estimate of helicity is based on the torsion angles ϕ and ψ of the peptide backbone. This expression was used to compute fractional helicity,

$$Helicity_{\text{torsions}} = \frac{\sum_{\phi,\psi} H^{\psi} \times H^{\phi}}{N^{\phi,\psi}}, \quad (4)$$

where $N^{\phi,\psi}$ is the number of ϕ,ψ dihedrals, and H^{ψ} is the helicity contribution from the torsion angle ψ defined as

$$H^{\psi} = \begin{cases} 1 & \text{for} \quad |\psi - \psi_o| \le a \\ 1 - \frac{(|\psi-\psi_o|-a)}{(b-a)} & \text{for} \quad a < |\psi - \psi_o| \le b \\ 0 & \text{for} \quad |\psi - \psi_o| > b \end{cases}. \quad (5)$$

A similar definition was used for H^{ϕ}. Based on the properties of a standard H-14 helix, we have used $\psi_o = -140°$, $\phi_o = -135°$, $a = 20°$, and $b = 39°$. Equation 4 implies that the helicity of the peptide is the sum of contributions from each of the backbone ϕ- and ψ-dihedral angles. Unlike the previous definition (Eq. 3), which assigns discrete values to helicity, Eqs. 4 and 5 provide a gradual estimate.

RESULTS AND DISCUSSION

Secondary structure formation in β-peptides

We begin by describing the results of molecular dynamics simulations of the three β-peptides in a distance-dependent dielectric continuum. It is experimentally known that β-peptides containing exclusively β^3-residues and/or ACHC residues exhibit a propensity to form 14-membered hydrogen bonds (6,33,34,43–46). Model H-14 helices were generated from the crystal structure of $[ACHC]_6$ in H-14 helical conformation (as shown in Fig. 3), and were used as initial conformations for the MD runs. These model helices were simulated in the presence of a distance-dependent dielectric with different values of α. Fig. 4 shows the time evolution of H-14 helicity, computed in two different ways (as discussed in Model and Methods) for $[\beta^3\text{hAla}]_{12}$ simulation starting with an initial conformation in a H-14 helical state. The β-peptide is able to maintain its H-14 conformation over a simulation time of 100 ns. It is also observed that, in some cases, denaturation at high temperatures followed by annealing leads to 12-membered hydrogen bonding in $[\beta^3\text{hAla}]_{12}$. Such H-12 helices have been reported as metastable (H-14 helix being the most stable) by earlier computational studies (19,25,29). Fig. 5 shows that, if started from an H-12 conformation, a simulation of $[\beta^3\text{hAla}]_{12}$ remains in that helical conformation over the entire duration of a long MD simulation. As mentioned earlier, the inability of MD simulations to sample the transformation of one helical structure into another, severely limits the usefulness of these calculations.

Increasing the polarity of the continuum solvent by raising the dielectric from $\alpha = 1.0$ to $\alpha = 1.2$ destabilizes both H-12 and H-14 helices. This is also in agreement with experimental results indicating that, compared to water, fewer polar solvents enhance the secondary structure of β-peptides. Note that lowering the Coulombic interactions by increasing α appears to destabilize the H-12 helix more than the H-14 helix (Fig. 4, *a* versus *b*). Earlier, Hofmann et al. (25) had reported results for β-peptides using the Gasteiger charges (CHARMM23.1 molecular mechanics force field), which are lower than the partial charges employed in this study. Our own exploratory runs with the Gasteiger charges reveal that lowering the charges severely destabilizes the H-12 population; H-14 is only marginally destabilized. These findings highlight the importance of electrostatic interactions in the stability of these peptides and also suggest that one may manipulate the secondary structure by tuning solvent quality.

Effect of dielectric on H-14 helicity

We now look more closely into the effect of the dielectric medium on the stability of H-14 helices for the three β-peptides. For the case of all-acyclic residues ($[\beta^3\text{hAla}]_{12}$), Fig. 6 *a* shows that while the H-14 helix is the stable structure for $\epsilon = 1.0\ r$ and $1.2\ r$, further increments of the dielectric strength lead to a disruption of the 14-membered hydrogen bond pattern. A similar behavior is seen for the one-third cyclic peptide,$[ACHC\text{-}\beta^3\text{Lys}\text{-}\beta^3\text{Leu}]_3$, as shown in Fig. 6 *b*.

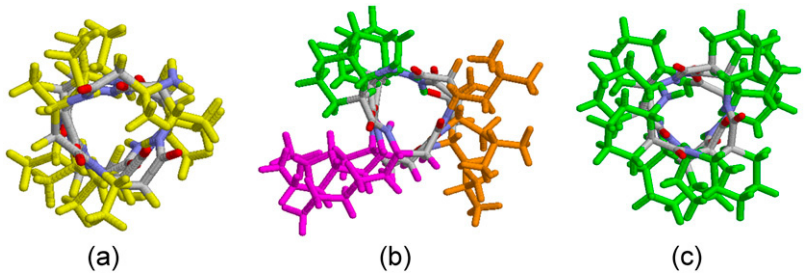

FIGURE 3 Schematic representation of three of the β-peptides in H-14 helical conformations: (*a*) all-acyclic $[\beta^3\text{hAla}]_{12}$; (*b*) one-third cyclic $[\beta^3\text{hAla}]_{12}$; and (*c*) all-cyclic residues $[ACHC]_9$.

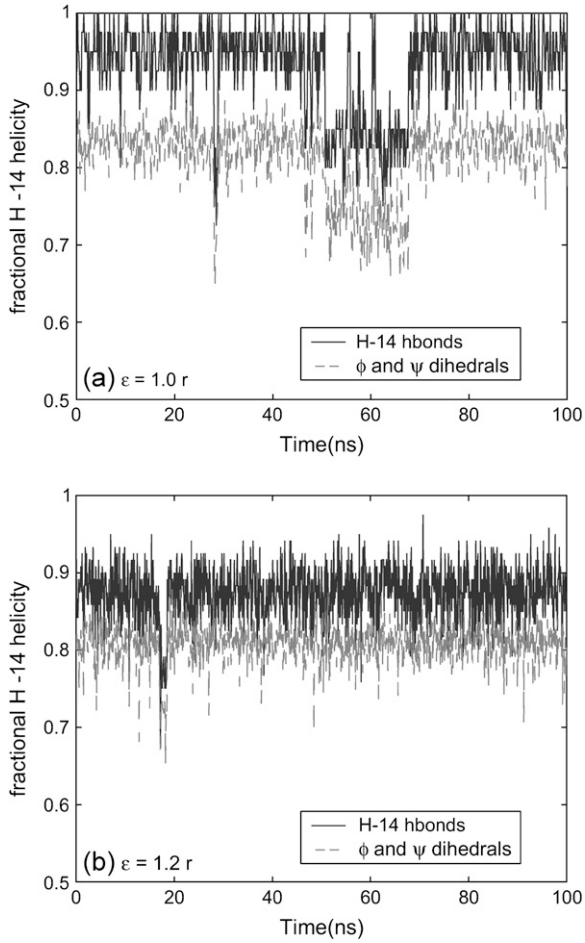

FIGURE 4 H-14 helicity of $[\beta^3\text{hAla}]_{12}$ in a continuum solvent using distance-dependent dielectric: (*a*) $\epsilon = 1.0\,r$ and (*b*) $\epsilon = 1.2\,r$. The solid lines correspond to H-14 helicity computed from the torsion angles and the dotted lines correspond to the estimate from the number of H-14 hydrogen bonds.

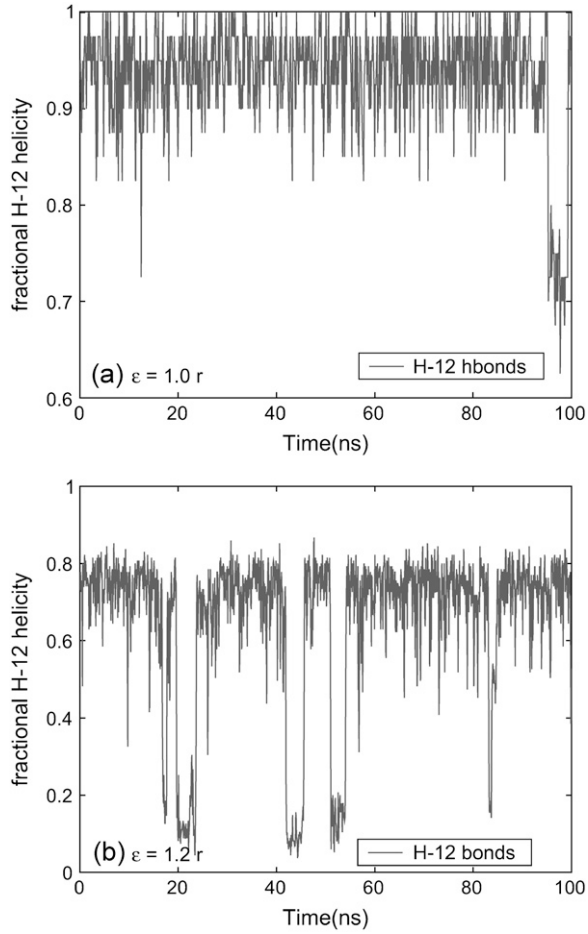

FIGURE 5 H-12 helicity of $[\beta^3\text{hAla}]_{12}$ in a continuum solvent using a distance-dependent dielectric: (*a*) $\epsilon = 1.0\,r$ and (*b*) $\epsilon = 1.2\,r$. Increasing the dielectric constant reduces the H-12 helicity to an extent greater than in the H-14 case. The helicity is estimated from the number of H-12 hydrogen bonds.

Compared to the acyclic case, the stability of the H-14 helix formed by the one-third cyclic peptide is enhanced, as the β-peptide is able to maintain its conformation in a more polar solvent ($\epsilon = 1.5\,r$). The use of all-cyclic residues, as in Fig. 6 *c*, further enhances H-14 stability. Even for the case of highest dielectric, the peptide maintains its H-14 helical conformation. This is consistent with the experimental findings (6,33,34) for β-peptides with *trans*-substituted cyclohexane rings (ACHC), where H-14 helicity is enhanced and the peptide can maintain its secondary structure in aqueous solvents. We are led to conclude that both H-14 and H-12 are stable helices under in-vacuo conditions, but are destabilized to a different extent in a polar solvent. These two helices differ in their dipole moment and the accessible surface area. The H-12-helix exhibits a smaller dipole moment and a larger surface area; it is more easily destabilized when the polarity of the solvent is increased. At the same time, the extent of H-14 helicity in a polar solvent can be increased by using steric interactions in the form of cyclic (six-membered) constraints.

Thermal stability of β-peptides in explicit solvent

MD runs in a continuum solvent predict that H-14 helix is the most stable conformation for the β-peptides. However, peptides comprising all-acyclic and one-third cyclic residues also exhibit metastable H-12 helices. We now explore the stability of these secondary structures in explicit solvents. Organic solvents are believed to enhance the secondary structures due to their reduced ability to hydrogen-bond with the peptide. To investigate this hypothesis, $[\beta^3\text{hAla}]_{12}$ was studied in explicit methanol. The use of cyclic residues can increase the H-14 helical propensity and help the peptides maintain their secondary structure in aqueous solution; we therefore simulate $[\text{ACHC}]_9$ and $[\text{ACHC-}\beta^3\text{Lys-}\beta^3\text{Leu}]_3$ in TIP3P water. The MD simulation runs are performed at two different temperatures.

Fig. 7 shows the time evolution of the root mean-square deviation (based on backbone α-carbon atoms) of the three peptides from their corresponding model H-14 helical states. At low temperatures, the three peptides are stable with respect

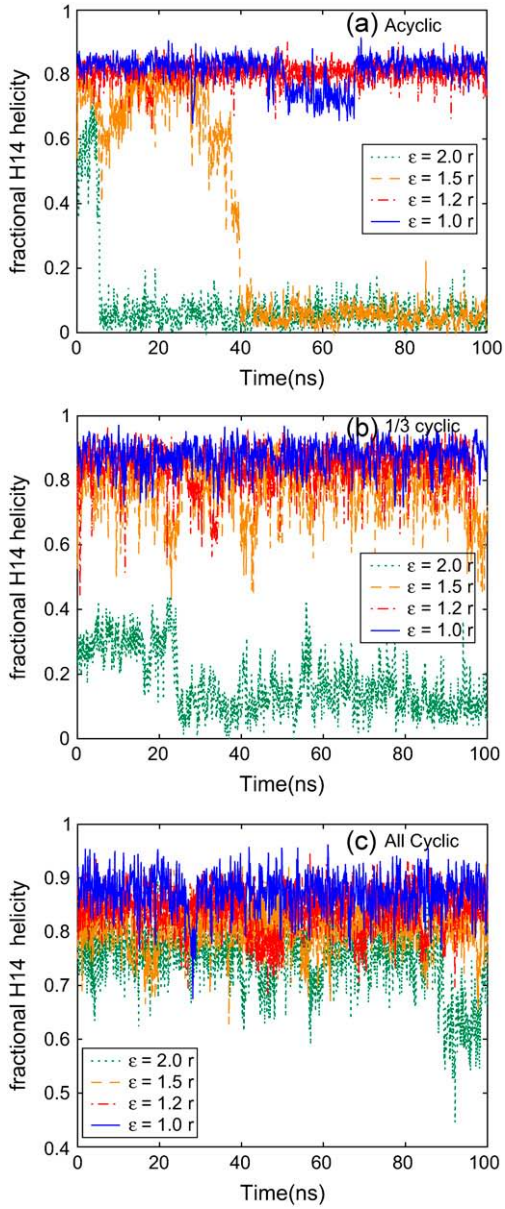

FIGURE 6 Effect of dielectric constant on the H-14 helical propensity of the three peptides. The H-14 conformations are stabilized more as the content of cyclic residues is increased.

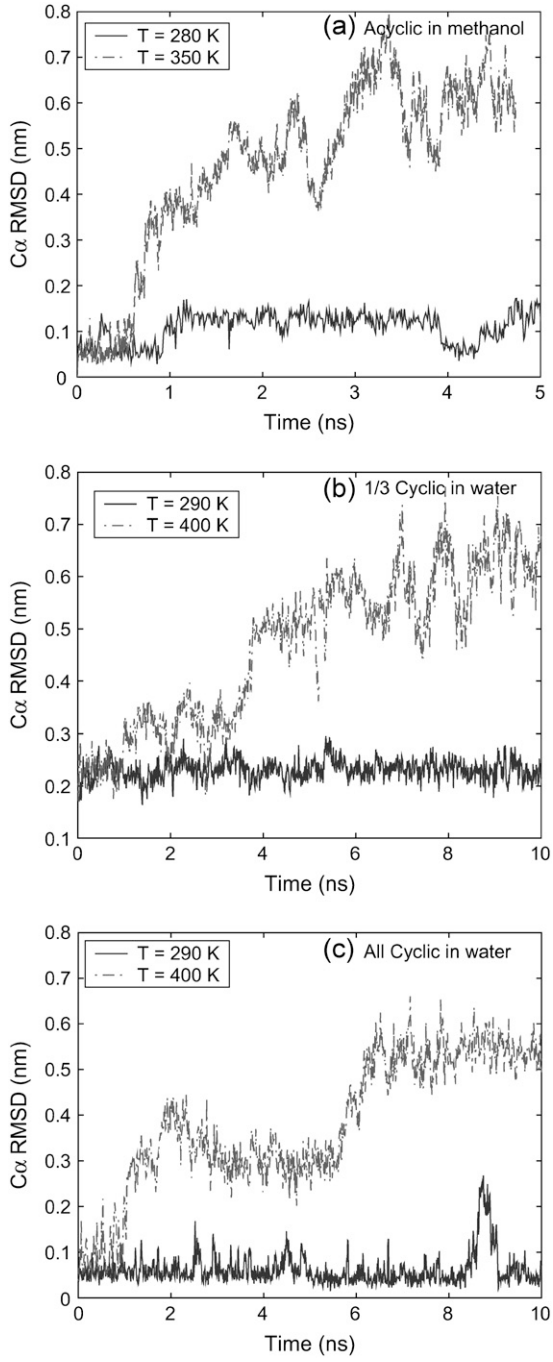

FIGURE 7 Root mean-square deviation from model H-14 helix computed based on C-α carbon atoms for the three β-peptides in explicit solvents: (*a*) acyclic; (*b*) one-third cyclic; and (*c*) all-cyclic residues.

to their H-14 states; minor deviations of the order of 1–3 Å arise from the movement of the free ends of the molecules (which are less stabilized due to insufficient hydrogen bonds on one side). The acyclic case of $[\beta^3\text{hAla}]_{12}$ is easily destabilized when the temperature is raised to 350 K. The other two β-peptides are more stable, with $[\text{ACHC}]_9$ exhibiting the highest stability at elevated temperatures of 400 K. This corroborates the experimental finding that ACHC-based cyclic residues enhance H-14 helical propensity.

We also examined the stability of the model H-12 helices in explicit solvents. Only the cases of all-acyclic and one-third cyclic residues exhibited 12-membered hydrogen-bonding as an alternate secondary structure in a distance-dependent dielectric. The all-cyclic case of $[\text{ACHC}]_9$ did not show any H-12 formation. We therefore investigated the stability of an H-12 conformer of $[\beta^3\text{hAla}]_{12}$ in explicit methanol at 280 K and that of $[\text{ACHC-}\beta^3\text{Lys-}\beta^3\text{Leu}]_3$ in explicit water at 290 K. Fig. 8 shows that the H-12 helical character of these two peptides disappears in <1 ns. Unlike their H-14 analogs, the

H-12 conformations are greatly destabilized by interactions with explicit solvent molecules. Note, however, that H-12 helices are unstable in methanol and water; but β-peptides containing acyclic residues could exhibit 12-membered hydrogen bonding in organic solvents of low polarity. Our distance-dependent dielectric calculations hint that organic solvents of low dielectric strength might stabilize the H-12 helices in the acyclic β^3-substituted peptides. While no such H-12 formation has been reported in the literature for these peptides, it is important to note that past experimental studies have relied on circular dichroism (CD) to monitor secondary structure formation in β-peptides. As mentioned earlier, CD is unable to unravel the existence of complex or mixed populations of folded structures. Fig. 9 shows calculated CD curves for pure H-14 and H-12 helices. Also shown are model CD spectra for mixed populations (H-14 + H-12) obtained by linear interpolation. The figure suggests that CD data only provide a qualitative view of secondary structure, and may not be able to identify low fractions (e.g., 15%) of H-12 population mixed in a pool of H-14 or vice versa.

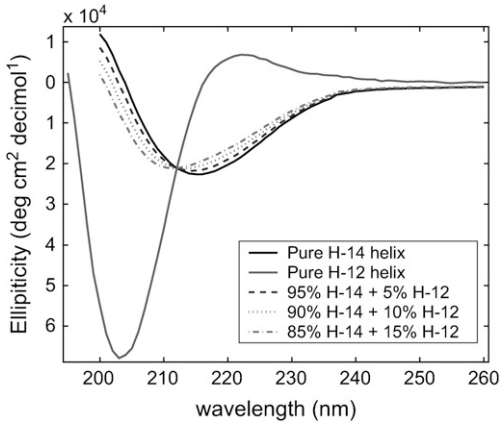

FIGURE 9 Model CD spectra for mixed populations.

EXEDOS on β-peptides

Although MD simulations provide an estimate of the stability of these peptides, their ability to sample configurational space is limited. Only when a structure is highly unstable (and therefore likely to disappear within a few nanoseconds) can MD runs provide some measure of stability. As shown in Figs. 4 and 5, MD simulations of low-energy, metastable structures are unable to escape from the starting conformation and are not capable of visiting neighboring minima on a timescale of 100 ns. To overcome this problem, in addition to molecular dynamics simulations, we use gas-phase density-of-states (EXEDOS) calculations (42) and investigate the role of dielectric constant on the relative stability of the two predominant helices: the H-12 and H-14. These two helices correspond to different optimal lengths, with H-12 being longer than the corresponding H-14 helix.

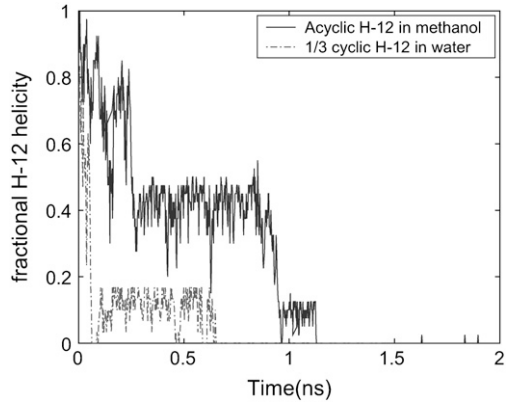

FIGURE 8 H-12 helicity for the β-peptide comprising all acyclic residues (*solid line*) and one-third cyclic residues (*dash-dot line*) in explicit solvent. The H-12 helices are unstable and quickly disappear in the presence of explicit solvent interactions.

The EXEDOS simulations are therefore performed in the end-to-end distance ensemble, as this clearly separates the H-12 population from the H-14. The results are obtained in the form of potentials of mean force (PMF) along the end-to-end distance. These PMF estimates are obtained to within an additive constant, and are therefore arbitrarily shifted on the y axis to match the values at the longest extension. This also provides an estimate of the mechanical strength (or extensional modulus) of these helices, a quantity that could be measured directly in single-molecule force spectroscopy. For each peptide (acyclic, one-third cyclic, and all-cyclic), simulations are conducted at two different dielectric strengths.

Figs. 10, 11, and 12 show the PMF obtained for the respective peptides and also the average secondary structure as a function of peptide length. The secondary structure is reported in terms of number of 14-membered and 12-membered hydrogen bonds being formed. Each of the peptides exhibits a pronounced minimum at an extension corresponding to the optimal length of an H-14 helix. For the case of acyclic and one-third cyclic peptides, in addition to the H-14 minimum, there is a weaker secondary minimum at the extension corresponding to an H-12 helix. This secondary minimum is weaker for the case of one-third cyclic than that for all-acyclic. The free energy difference between H-12 and H-14, which is ~14.4 kJ/mol for $[\beta^3\text{hAla}]_{12}$, increases to an ~24.8 kJ/mol upon incorporation of one-third cyclic residues. To be consistent with respect to chain length and amino-acid side chains, similar EXEDOS computations were also performed on $[\beta^3\text{hAla}]_9$ and $[\text{ACHC-}\beta^3\text{hAla-}\beta^3\text{hAla}]_3$. For the peptide ($[\beta^3\text{hAla}]_9$), reducing the chain length resulted in a reduction of the free energy difference between the two populations (H-12 and H-14) to ~8 kJ/mol. For the one-third cyclic case, $[\text{ACHC-}\beta^3\text{hAla-}\beta^3\text{hAla}]_3$ led to a free energy difference of ~12.5 kJ/mol, consistent with its reduced propensity toward H-14 formation as compared to $[\text{ACHC-}\beta^3\text{Lys-}\beta^3\text{Leu}]_3$. The all-cyclic case of $[\text{ACHC}]_9$

does not exhibit an H-12 minimum, and the only stable conformation is the H-14 helix. These results confirm that use of ACHC-based cyclic constraints enhances H-14 propensity and destabilizes H-12 formation. When the dielectric constant of the continuum solvent is increased, the secondary structures become less stable. Even though the free energy difference between the H-14 and H-12 helix is reduced, H-12 helices are easier to disrupt because they correspond to a weaker free-energy minimum. This is consistent with the results of molecular dynamics simulations shown in Fig. 4.

The free energy profiles determined in this work suggest that, in high polarity solvents, the all-cyclic molecules fold rapidly and directly into the H-14 conformation. In contrast, in lower polarity solvents and for lesser cyclic contents, the β-peptides considered in this work could also fold in a two-step process, first reaching an H-12 conformation and then adopting an H-14 conformation. These ideas will be explored by means of transition-path ensemble simulations in future work.

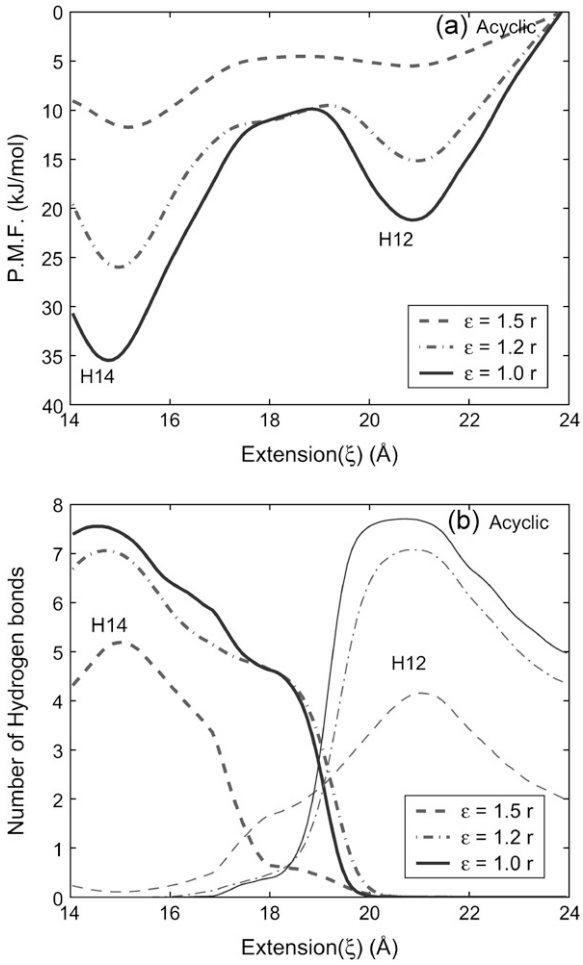

FIGURE 10 (*a*) Potential of mean force associated with end-to-end distance of the acyclic β-peptide, $[\beta^3\text{hAla}]_{12}$. (*b*) Number of H-14 and H-12 hydrogen bonds as a function of peptide extension. The two minima in the PMF correspond to H-14 conformations (shorter ξ) and H-12 conformations (longer ξ). Different curves correspond to different dielectric constants.

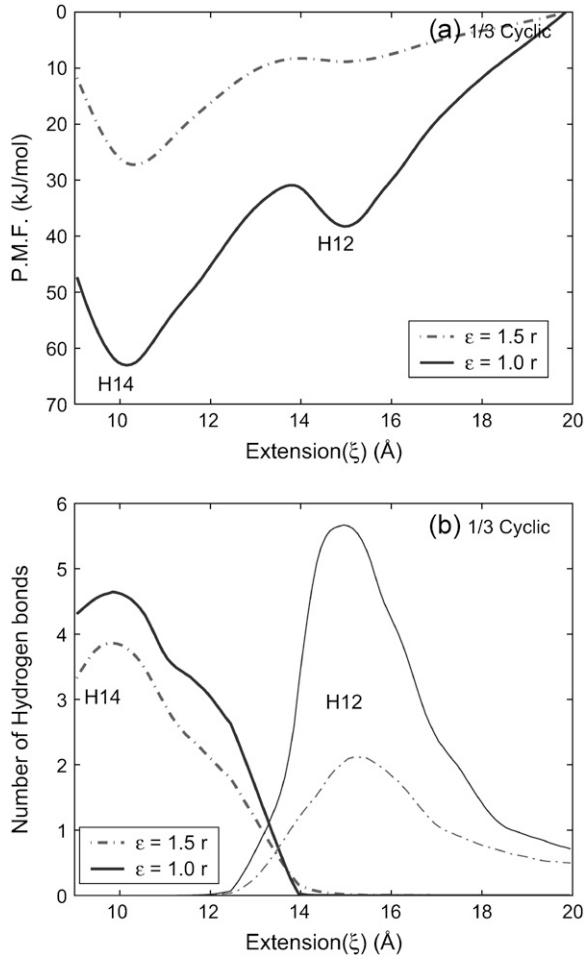

FIGURE 11 (*a*) Potential of mean force associated with end-to-end distance of the one-third cyclic β-peptide, $[\beta^3\text{hAla}]_{12}$. (*b*) Number of H-14 and H-12 hydrogen bonds as a function of peptide extension. The two minima in the PMF correspond to H-14 conformations (shorter ξ) and H-12 conformations (longer ξ).

Effect of cyclic residues

The main difference between the structural properties of the H-12 and H-14 helices lies in the torsion angle, θ (see Fig. 1 for definition). While θ is equal to 60° for the case of a model H-14 helix, it is ~95° for an H-12 helix (the sign may differ depending on the chirality of the molecule). The use of *trans*-substituted cyclohexane rings (ACHC) places constraints on the peptide backbone and forces the θ-value to be 60°. As a result, the H-12 helix is greatly destabilized. In addition, cyclic residues make the stability of H-14 less dependent on the electrostatic interactions. The peptide is now stabilized by the favorable dihedral angle potential. Therefore, changing the solvent from less polar to an aqueous solution has a smaller effect on the H-14 helicity of cyclic peptides than that of their acyclic analogs.

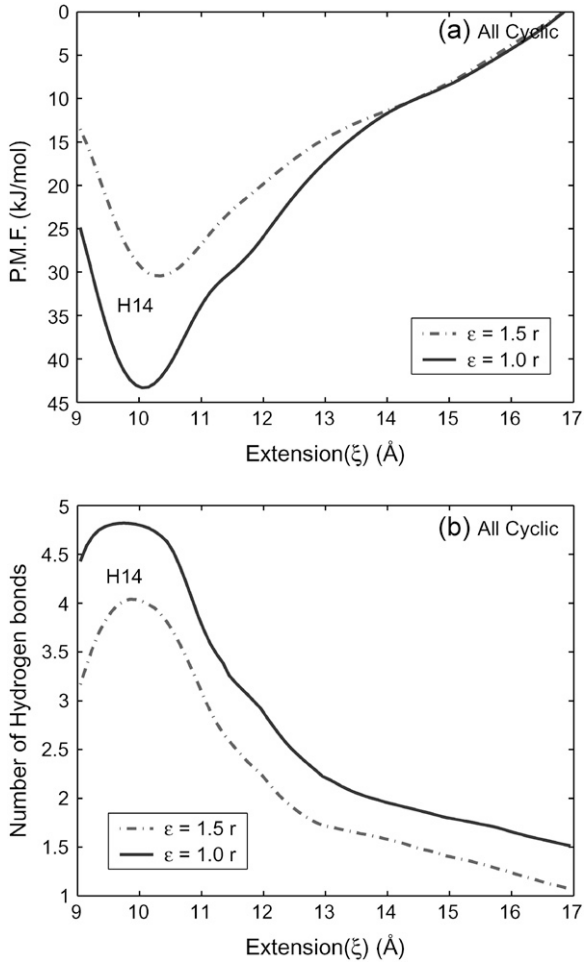

FIGURE 12 (*a*) Potential of mean force associated with end-to-end distance of the all-cyclic β-peptide, $[ACHC]_9$. (*b*) Number of H-14 and H-12 hydrogen bonds as a function of peptide extension. Unlike the other two peptides there is only one minimum in the PMF corresponding to H-14 conformation.

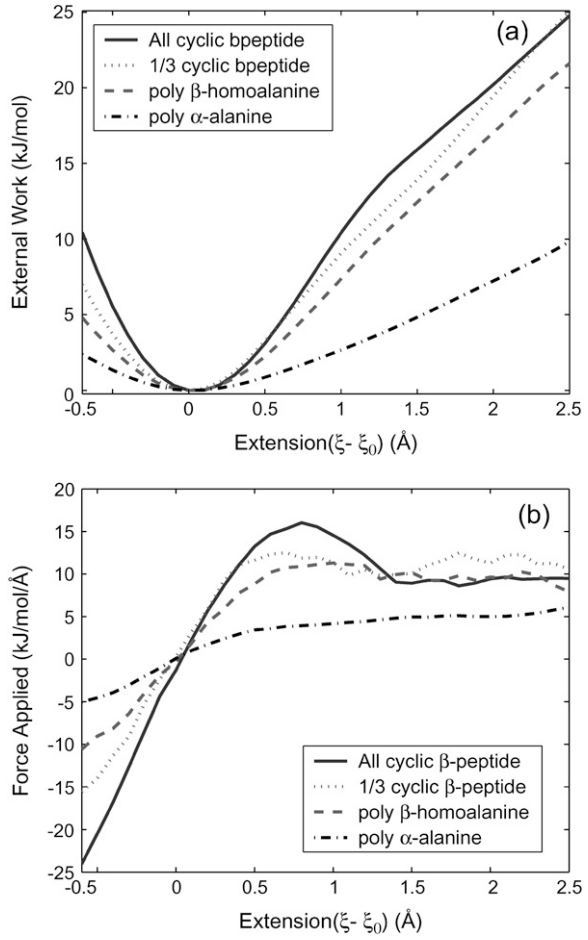

FIGURE 13 Comparison of mechanical strength of different peptides. (*a*) External work and (*b*) external force needed to stretch the four peptides from their optimal end-to-end distance. The H-14 helix formed by β-peptides has greater mechanical strength than the conventional α-helix.

Comparison of mechanical strength of α- and β-peptides

In an earlier study (42), we presented results of EXEDOS calculations on a united-atom model of poly(α)-alanine. Short oligomers of α-alanine were shown to form stable α-helices in the presence of a distance-dependent dielectric and an implicit solvent based on the accessible surface area of the peptide (39). The calculations for β-peptides presented in this work were performed with an all-atom model, which is slightly different than that employed for α-alanine. These differences not withstanding, it is of interest to compare the mechanical strength of the α-helix formed by 15-mer α-alanine and the H-14 helices formed by the three peptides studied in this work. In Fig. 13 we compare the amount of 1), external work; and 2), external force needed to stretch different helices from their optimal lengths, ξ_0. The figure shows that the H-14 helices formed by β-peptides are mechanically stronger than an α-helix of comparable length. This could prove to be a significant design feature in favor of β-peptides for peptidomimetic applications. Within the limits of errors associated with these calculations, we can also conclude that the use of cyclic residues further enhances the mechanical strength of these peptides.

CONCLUSION

We have presented a detailed computational analysis of the thermodynamic stability of β-peptides in the context of single-molecule force spectroscopy, both in a dielectric continuum and in explicit solvents. We have examined in a systematic manner the effect of cyclic residue content on β-peptide stability and conformation. In contrast to earlier computational studies that relied on potential energy minimization or molecular dynamics simulations, our density-of-states based Monte Carlo simulations have revealed the existence of distinct populations of folded structures.

Furthermore, our calculations have generated unambiguous, high-accuracy estimates of the free energy and relative stability of the two predominant populations of helices. Even though optimization of the force-field parameters for these synthetic amino acids remains an open area of research, we have shown that CHARMM-like parameters can be used to explain many of the experimentally observed behaviors of cyclic-substituted β-peptides. Cyclic residues are found to enhance H-14 helicity in the β^3-peptides and make them more stable in aqueous solution. The dielectric constant of the medium plays a key role in governing the stability of H-12 and H-14 secondary structures. Our results suggest that the quality of the solvent can be used to manipulate hydrogen-bonding patterns in these molecules. The H-12 helices have a smaller dipole moment and are more easily destabilized in a polar solvent. At the same time, use of cyclic constraints can be exploited to render H-14 helices more robust and less sensitive to solvent polarity. Interestingly, comparison of the mechanical strength of cyclic-residue substituted β-peptides shows that the helical structures adopted by these molecules are more mechanically stable than those formed by α-amino-acid oligomers.

The results of our calculations indicate that single-molecule force spectroscopy could probe unambiguously the relative stability and free energy of the various conformations assumed by β-peptide foldamers. Furthermore, preliminary calculations reveal that such conformations could be highly sensitive to foldamer concentration. The free energy profiles determined in this work will now be used to examine the folding process of β-peptides by means of transition-path ensemble simulations. Plans are currently underway to measure the reversible work required to unfold distinct molecules.

The authors are grateful to Prof. H.-J. Hofmann of the Institute of Biochemistry, Leipzig, for useful discussions and valuable suggestions. We are also grateful to Will Pomerantz and Justin Murray for sharing their insights about β-peptide behavior.

This work was supported by the National Science Foundation through the University of Wisconsin Nanoscale Science and Engineering Center (DMR 0425880).

REFERENCES

1. Gellman, S. H. 1998. Foldamers: a manifesto. *Acc. Chem. Res.* 31: 173–180.
2. Hill, D. J., M. J. Mio, R. B. Prince, T. S. Hughes, and J. S. Moore. 2001. A field guide to foldamers. *Chem. Rev.* 101:3893.
3. Huc, I. 2004. Aromatic oligoamide foldamers. *Eur. J. Org. Chem.* 1:17–29.
4. Cheng, R. P., S. H. Gellman, and W. F. DeGrado. 2001. β-peptides: from structure to function. *Chem. Rev.* 101:3219–3232.
5. Seebach, D., A. K. Beck, and D. J. Bierbaum. 2004. The world of β- and γ-peptides comprised of homologated proteinogenic amino acids and other components. *Chem. Biodivers.* 1:1111–1239.
6. Appella, D. H., J. J. J. Barchi, S. R. Durell, and S. H. Gellman. 1999. Formation of short, stable helices in aqueous solution by β-amino acid hexamers. *J. Am. Chem. Soc.* 121:2309–2310.
7. Wang, X., J. F. Espinosa, and S. H. Gellman. 2000. 12-helix formation in aqueous solution with short β-peptides containing pyrrolidine-based residues. *J. Am. Chem. Soc.* 122:4821–4822.
8. Lee, H. S., F. A. Syud, X. Wang, and S. H. Gellman. 2001. Diversity in short β-peptide 12-helices: high resolution structural analysis in aqueous solution of a hexamer containing sulfonylated pyrrolidine residues. *J. Am. Chem. Soc.* 123:7721–7722.
9. Chakrabarty, A., and R. L. Baldwin. 1995. Stability of α-helices. *Adv. Protein Chem.* 46:141–176.
10. Raguse, T. L., J. R. Lai, and S. H. Gellman. 2003. Environment-independent 14-helix formation in short β-peptides: striking a balance between shape control and functional diversity. *J. Am. Chem. Soc.* 125:5592–5593.
11. Apella, D. H., L. A. Christianson, D. Klein, D. R. Powell, X. Huang, J. J. Barchi, and S. H. Gellman. 1997. Residue-based control of helix shape in β-peptide oligomers. *Nature.* 387:381.
12. Frackenpohl, J., P. I. Arvidsson, J. V. Schreiber, and D. Seebach. 2001. The outstanding biological stability of β- and γ-peptidases. *ChemBioChem.* 2:445–455.
13. Werder, M., S. Abele, and D. Seebach. 1999. Beta-peptides as inhibitors of small-intestinal cholesterol and fat absorption. *Helv. Chim. Acta.* 82:1774–1783.
14. Hamuro, Y., J. P. Schneider, and W. L. DeGrado. 1999. De novo design of antibacterial β-peptides. *J. Am. Chem. Soc.* 121:12200–12201.
15. Porter, E. A., X. Wang, H. S. Lee, B. Weisblum, and S. H. Gellman. 2000. Antibiotics: non-haemolytic β-amino acid oligomers. *Nature.* 404:565.
16. Kritzer, J. A., N. W. Luedtke, E. A. Harker, and A. Schepartz. 2005. A rapid library screening for tailoring β-peptide structure and function. *J. Am. Chem. Soc.* 127:14584–14585.
17. Stephens, O. M., S. Kim, B. D. Welch, M. E. Hodsdon, M. S. Kay, and A. Schepartz. 2005. Inviting HIV fusion with a β-peptide foldamer. *J. Am. Chem. Soc.* 127:13126–13127.
18. English, E. P., R. S. Chumanov, S. H. Gellman, and T. Compton. 2006. Rational development of β-peptide inhibitors of human cytomegalovirus entry. *J. Biol. Chem.* In press.
19. Wu, Y.-D., and D.-P. Wang. 1998. Theoretical studies of β-peptide models. *J. Am. Chem. Soc.* 120:13485–13493.
20. Daura, X., W. F. van Gunsteren, and A. E. Mark. 1999. Folding-unfolding thermodynamics of a β-heptapeptide from equilibrium simulations. *Proteins Struct. Funct. Genet.* 34:269–280.
21. Daura, X., K. Gademann, H. Schafer, B. Jaun, D. Seebach, and W. F. van Gunsteren. 2001. The β-peptide hairpin in solution: conformational study of a β-hexapeptide in methanol by NMR spectroscopy and MD simulation. *J. Am. Chem. Soc.* 123:2393–2404.
22. Schafer, H., X. Daura, A. E. Mark, and W. F. van Gunsteren. 2001. Entropy calculations on a reversibly folding peptide: changes in solute free energy cannot explain folding behavior. *Proteins Struct. Funct. Genet.* 43:45–56.
23. Glattli, A., D. Seebach, and W. F. van Gunsteren. 2004. Do valine side chains have an influence of folding behavior of β-substituted β-peptides? *Helv. Chim. Acta.* 87:2487–2506.
24. Mohle, K., R. Gunther, M. Thormann, N. Sewald, and H.-J. Hofmann. 1999. Basic conformers in β-peptides. *Biopolymers.* 50:167–184.
25. Gunther, R., and H.-J. Hofmann. 2001. Searching for periodic structures in β-peptides. *J. Phys. Chem. B.* 105:5559–5567.
26. Gunther, R., and H.-J. Hofmann. 2002. Theoretical prediction of substituent effects on the intrinsic folding properties of β-peptides. *Helv. Chim. Acta.* 85:2149–2168.
27. Jorgensen, W. L., D. S. Maxwell, and J. Tirado-Rives. 1996. Development and testing of the OPLS all-atom force field on conformational energetics and properties of organic liquids. *J. Am. Chem. Soc.* 118: 11225–11236.
28. Chandrasekhar, J., M. Saunders, and W. L. Jorgensen. 2001. Efficient exploration of conformational space using the stochastic search method: application to β-peptide oligomers. *J. Comput. Chem.* 22:1646–1654.

29. Kritzer, J. A., J. Tirado-Rives, S. A. Hart, J. D. Lear, W. L. Jorgensen, and A. Schepartz. 2005. Relationship between side-chain structure and 14-helix stability of β^3-peptides in water. *J. Am. Chem. Soc.* 127: 167–178.

30. Li, H., A. F. Oberhauser, S. B. Fowler, J. Clarke, and J. M. Fernandez. 2000. Atomic force microscopy reveals the mechanical design of a modular protein. *Proc. Natl. Acad. Sci. USA.* 97:6527–6531.

31. Kellermayer, M. S. Z., S. B. Smith, H. L. Granzier, and C. Bustamante. 1997. Folding-unfolding transition in single titin modules characterized with laser tweezers. *Science.* 276:1112–1116.

32. Bryant, Z., M. D. Stone, J. Gore, S. B. Smith, N. R. Cozzarelli, and C. Bustamante. 2003. Structural transitions and elasticity from torque measurements on DNA. *Nature.* 424:338–341.

33. Appella, D. H., L. A. Christianson, I. L. Karle, D. R. Powell, and S. H. Gellman. 1996. β-peptide foldamers: robust helix formation in a new family of β-amino acid oligomers. *J. Am. Chem. Soc.* 124:13071–13072.

34. Appella, D. H., L. A. Christianson, I. L. Karle, D. R. Powell, and S. H. Gellman. 1999. Synthesis and characterization of *trans*-2-aminocyclohexanecarboxylic acid oligomers: an unnatural helical secondary structure and implications for β-peptide tertiary structure. *J. Am. Chem. Soc.* 121:6206–6212.

35. MacKerrell, Jr., A. D., D. Bashford, M. Bellott, R. L. Dunbrack, J. D. Evanseck, M. J. Field, S. Fischer, J. Gao, H. Guo, S. Ha, D. Joseph-McCarthy, L. Kuchnir, K. Kuczera, F. T. K. Lau, C. Mattos, S. Michnick, T. Ngo, D. T. Nguyen, B. Prodhom, W. E. Reiher, B. Roux, M. Schlenkrich, J. C. Smith, R. Stote, J. Straub, M. Watanabe, J. Wiorkiewicz-Kuczera, D. Yin, and M. Karplus. 1998. All-atom empirical potential for molecular modeling and dynamics studies of proteins. *J. Phys. Chem. B.* 102:3586–3617.

36. Essmann, U., L. Perera, M. L. Berkowitz, T. Darden, H. Lee, and L. G. Pederson. 1995. A smooth particle mesh Ewald method. *J. Chem. Phys.* 103:8577–8593.

37. Jorgensen, W. L., J. Chandrasekhar, J. D. Madura, R. W. Impey, and M. L. Klein. 1983. Comparison of simple potential functions for simulating liquid water. *J. Chem. Phys.* 79:926–935.

38. Peng, Y., and U. H. E. Hansmann. 2002. Solvation model dependency of helix-coil transition in polyalanine. *Biophys. J.* 82:3269–3276.

39. Ferrara, P., J. Apostolakiz, and A. Caflisch. 2002. Evaluation of a fast implicit solvent model for molecular dynamics simulations. *Proteins Struct. Funct. Genet.* 46:24–33.

40. Martyna, G. J. 1996. Explicit reversible integrators for extended systems dynamics. *Mol. Phys.* 87:1117–1157.

41. Kim, E. B., R. Faller, Q. Yan, N. L. Abbott, and J. J. de Pablo. 2002. Potential of mean force between a spherical particle suspended in a nematic liquid crystal and a substrate. *J. Chem. Phys.* 117:7781–7787.

42. Rathore, N., Q. Yan, and J. J. de Pablo. 2004. Molecular simulation of the reversible mechanical unfolding of proteins. *J. Chem. Phys.* 120: 5781–5788.

43. Seebach, D., M. Overhand, F. N. M. Kuhnle, B. Martinoni, L. Oberer, U. Hommel, and H. Widmer. 1996. β-peptides: synthesis by Arndt-Eistert homologation with concomitant peptide coupling. Structure determination by NMR and CD spectroscopy and by x-ray crystallography. Helical secondary structure of a β-hexapeptide in solution and its stability towards pepsin. *Helv. Chim. Acta.* 79:913–941.

44. Seebach, D., and J. L. Matthews. 1997. β-peptides: a surprise at every turn. *Chem. Commun.* 2015–2022.

45. Appella, D. H., L. A. Christianson, D. A. Klein, M. R. Richards, D. R. Powell, and S. H. Gellman. 1999. Synthesis and structural characterization of helix-forming β-peptides: *trans*-2-aminocyclopentanecarboxylic acid oligomers. *J. Am. Chem. Soc.* 121:6206–6212.

46. Applequist, J., K. A. Bode, D. H. Apella, L. A. Christianson, and S. H. Gellman. 1998. Theoretical and experimental circular dichroic spectra of the novel helical foldamer poly[(1*r*,2*r*)-*trans*-2-aminocyclopentanecarboxylic acid]. *J. Am. Chem. Soc.* 120:4891–4892.